Scientific Research Publishing

Open Journal of Optimization, 2025, 14(4), 131-146
https://www.scirp.org/journal/ojop
ISSN Online: 2325-7091
ISSN Print: 2325-7105

A Nonlinear Mathematical Model for Dynamic Traffic Flow Optimization: A Stem Innovation

Marc Bigirimana[1*], Fulgence Nahayo[1], Mounir Haddou[2], Abraham Niyongere[3]

[1]Laboratoire Universitaire de Recherche en Modélisation et en Ingénierie de Statistique Appliquée, Université du Burundi, Bujumbura, Burundi
[2]Institut de Recherche Mathématique de Rennes/Institut National des Sciences Appliquées de Rennes, Université de Rennes, Rennes, France
[3]Centre de Recherche en Infrastructures, Environnement et Technologie, Université du Burundi, Bujumbura, Burundi
Email: *marc.bigirimana@ub.edu.bi, fulgence.nahayo@ub.edu.bi, Mounir.Haddou@insa-rennes.fr, abraham.niyongere@ub.edu.bi

How to cite this paper: Bigirimana, M., Nahayo, F., Haddou, M. and Niyongere, A. (2025) A Nonlinear Mathematical Model for Dynamic Traffic Flow Optimization: A Stem Innovation. *Open Journal of Optimization*, **14**, 131-146.
https://doi.org/10.4236/ojop.2025.144008

Received: August 20, 2025
Accepted: October 26, 2025
Published: October 29, 2025

Abstract

This paper aims to develop a model of road traffic dynamics. The Heat-powered vehicle is modeled as a highly complex, controlled dynamic system whose 3D motion considers kinematic, dynamic, and rotational contributions. An objective function to optimize traffic flow is proposed. An additional assumption of mass variation of the thermal vehicle in motion is added to the fundamental principle of dynamic mechanics formulated by Sir Isaac Newton. A set of constraints related to dynamics, kinematics, control, and comfort is taken into consideration. A set of intercoupled nonlinear differential equations governs the formulation of this problem. A Runge-Kutta discretization RK4 is required to solve the problem. A Mathematical Programming Language AMPL and the Interior Point OPTimizer IPOPT solver are used to extract solutions. The numerical results confirm the assumption of mass variation and a considerable improvement in traffic fluidity.

Keywords

Traffic Fluidity Function, Mass Variation, AMPL, IPOPT, Inter-Coupled Differential Equations, RK4 Discretization, Heat-Powered Vehicle

1. Introduction

The problem of planning, managing, and optimizing road traffic takes as its starting point the modeling of various systems involving the maintenance of state and

the control of vehicle movement. Overall, road Traffic is made up of two components such as the road infrastructure and the mobiles.

To gain a deeper understanding of the vehicle on the road infrastructure, we wish to optimize safe driving conditions; the vehicle system modeling stage is fundamental [1].

Here are two aims of this work. Firstly, to meet the growing demand for road infrastructure capacity through the efficient or optimal use of existing road infrastructure. This means optimizing the inverse function of road congestion, also known as the traffic fluidity function [2] [3]. On the other to establish the dynamic equations characterizing the temporal evolution of the various variables involved in the dynamic modeling of the thermal vehicle system. This means knowledge of a mathematical model made up of a set of differential equations of motion representing physical phenomena is necessary for the representation and analysis of vehicle dynamics and the design of control laws, comfort, and safety [4]. The thermal vehicle interacts with the external environment through the driver and the road. Both play an important role but are difficult to control.

In this paper, we study the overall motion of the thermal vehicle with all its components. For acceleration and braking movements, it is often important to consider the vehicle as a rigid body, characterized by its center of mass, its mass, and its tensor of inertia of the moments of external forces [4] [5]. The model developed in this work is a complex, controlled nonlinear problem, leading to a system of inter-coupled nonlinear differential equations. A nonlinear software, namely Interior Point OPTimizer solver coupled with AMPL, is used to extract optimal dynamic solutions of the nonlinear problem of road traffic optimization. Matlab software is used as an interface for graphical visualization of optimal solutions.

The dynamic system of these nonlinear differential equations, the road traffic fluidity function and the numerical 4th-order Runge-Kutta discretization method are presented in sections 2 and 3, respectively, while the numerical results are presented in section 4.

2. Mathematical Formulation of the Road Traffic

In this section, we model the dynamics of heat-powered vehicle and traffic flow function to be optimized.

Here, the thermal vehicle is considered as a rigid solid with a fixed center of gravity and a variable mass when moving [6]. The equations of motion of a rigid body are obtained from Newton's second law. The variation in mass can be due to several factors influencing the vehicle system, such as engine propulsion, fuel consumption, and the addition of driver, passengers, and luggage, all of which have a non-negligible effect on the total mass of the vehicle.

The vehicle is then modeled as a highly complex dynamic system taking into account translation and rotational movements and its dynamics are influenced by the contributions of aerodynamic drag forces, longitudinal forces, frictional forces and gravitational forces. See **Figure 1** [7].

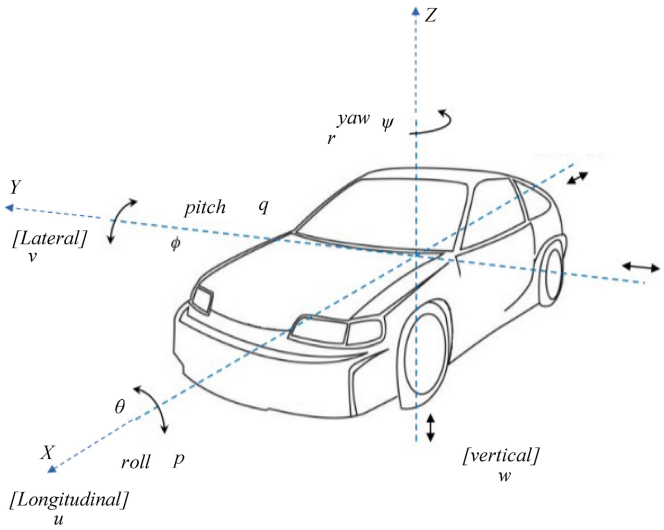

Figure 1. An overview of the three-dimensional movement of the vehicle body [7].

2.1. Dynamic Modelling of Thermal Vehicle System

Various reference frames can be employed for the modeling and analysis of the motion of vehicle, but in reality, three reference frames are used to derive the equations of motion for vehicle mechanics [8]. Now, the 3D motion of the thermal vehicle is then studied in three 3D reference frames, respectively called the mobile frame $R_G\left(G, X_G, Y_G, Z_G\right)$ associated with the vehicle's center of gravity G; aerodynamic frame R_a and the inertial frame fixed to the ground $R_O\left(O, X_O, Y_O, Z_O\right)$. The transition from the inertial frame R_O to the moving frame R_G is carried by a matrix R known as the rotation operator [5] [6].

The equations describing the dynamics of the thermal vehicle system are summarized in Isaac Newton's two principles, to which we add the hypothesis of variation in the mass of the moving vehicle [1] [9]:

$$\sum F_{ext} - \frac{\mathrm{d}m}{\mathrm{d}t} v_a = m\dot{v}_a, \quad \sum M_{F_{ext}} = J\left(G, V_{eh}\right)\frac{\mathrm{d}\Omega}{\mathrm{d}t} \tag{1}$$

In the above system, F_{ext} are the external forces acting on the moving vehicle, $m(t)$ is the mass of the vehicle, v_a is the aerodynamic speed of the vehicle, $J\left(G, V_{eh}\right)$ is the inertial matrix of the vehicle and Ω is the rotation speed vector of the vehicle in three directions, as shown in **Figure 1**.

The relations between the derivatives in the R_G frame and R_O are given by the following fundamental relation of dynamics or Poisson's formula [9] [10]:

$$\left.\frac{\mathrm{d}\mathbf{r}}{\mathrm{d}t}\right|_{R_O} = \left.\frac{\mathrm{d}\mathbf{r}}{\mathrm{d}t}\right|_{R_G} + \boldsymbol{\Omega}_{R_G/R_O} \wedge \mathbf{r} \tag{2}$$

where $\left.\frac{\mathrm{d}\mathbf{r}}{\mathrm{d}t}\right|_{R_O}$ is the derivative with respect to time of the vector $\mathbf{r}$ in the inertial frame R_O, $\left.\frac{\mathrm{d}\mathbf{r}}{\mathrm{d}t}\right|_{R_G}$ is the derivative with respect to time of the vector $\mathbf{r}$ in the vehicle frame R_G, $\boldsymbol{\Omega}$ is the angular velocity of the vehicle and $\boldsymbol{\Omega}_{R_G/R_O}$ is the

angular velocity R_G with respect to R_O [9].

The relation (2) means that the derivation is made considering an observatory attached to the R_O frame but the equations are written in the R_G frame. A second-time derivation and then multiplying the two members of the fundamental Equation (2) by the mass $m(t)$ of the vehicle, and under the additional assumption that the mass of the vehicle varies only in the R_G frame, we obtain the following dynamic system:

$$
\begin{cases}
\dot{m} = -\left(C_{cse} \times \tau \times \left[\dfrac{P_i v_e}{LHV_{fuel} \cdot \eta_m \cdot \eta_c} + (p_0 - p_e) \cdot A_e \right] \right)^{\frac{1}{2}} \\
\dot{v}_a = \dfrac{1}{2m} \rho A_f C_a \left(v_a + v_{wind} \right)^2 + C_r g \cos\theta \\
\dot{\gamma}_a = -\dfrac{\dot{m}}{2m^2} \rho A_f C_a \left(v_a + v_{wind} \right)^2 + \dfrac{1}{m} \rho A_f C_a \dot{v}_a \left(v_a + v_{wind} \right) - C_r g \dot{\theta} \sin\theta \\
\dot{u} = \dfrac{1}{m} \left[-mg \sin\theta - \dfrac{1}{2} \rho A_f \left(u + u_w \right)^2 C_x - C_r mg \cos\theta + F_x - \dot{m} u - m(qw - rv) \right] \\
\dot{v} = \dfrac{1}{m} \left[mg \cos\theta \sin\phi + \dfrac{1}{2} \rho A_f \left(v + v_w \right)^2 C_y + F_y - \dot{m} v - m(ru - pw) \right] \\
\dot{w} = \dfrac{1}{m} \left[mg \cos\theta \cos\phi + \dfrac{1}{2} \rho A_f \left(w + w_w \right)^2 C_z + F_z - mg \cos\theta - \dot{m} w - m(pv - qu) \right] \\
\dot{p} = \dfrac{C}{AC - D^2} \left[\dfrac{1}{2} \rho A_f t \left(u + u_w \right)^2 C_l + (B - C) qr + Dpq \right] \\
\quad + \dfrac{D}{AC - D^2} \left[\dfrac{1}{2} \rho A_f L \left(w + w_w \right)^2 C_n + (A - B) pq - Dqr \right] \\
\dot{q} = \dfrac{1}{B} \left[\dfrac{1}{2} \rho A_f L \left(v + v_w \right)^2 C_m + (C - A) pr - D\left(p^2 - r^2 \right) \right] \\
\dot{r} = \dfrac{A}{AC - D^2} \left[\dfrac{1}{2} \rho A_f L \left(w + w_w \right)^2 C_n + (A - B) pq - Dqr \right] \\
\quad + \dfrac{D}{AC - D^2} \left[\dfrac{1}{2} \rho A_f t \left(u + u_w \right)^2 C_l + (B - C) qr + Dpq \right] \\
\dot{\phi} = p + q \tan\theta \sin\phi + r \tan\theta \cos\phi, \dot{\theta} = q \cos\phi - r \sin\phi, \\
\dot{\psi} = q \dfrac{\sin\phi}{\cos\theta} + r \dfrac{\cos\phi}{\cos\theta} \\
\dot{X}_G^o = u \cos\psi - v \sin\psi, \dot{Y}_G^o = u \cos\psi + v \sin\psi, \dot{Z}_G^o = w
\end{cases}
\tag{3}
$$

where ψ, θ and ϕ are yaw, roll and pitch angles of the vehicle. $A = I_{xx}$, $B = I_{yy}$, $C = I_{zz}$ and $D = I_{xz}$ are the moments of inertia of the vehicle. C_{cse} is the specific consumption coefficient of the vehicle. τ and v_e are respectively the coefficient of performance and the gas ejection velocity relative to the engine. P_i is the power injected into the engine, LHV_{fuel} is the calorific power of the fuel. η_m and η_c are respectively the engine's mechanical efficiency and the fuel's combustion efficiency, p_e and p_0 are respectively the exhaust gas pressure at the engine outlet and the ambient atmospheric pressure. A_e is the exhaust gas surface area, ρ is the air density, A_f is the frontal area of the vehicle and t is the vehicle width [11] [12]. C_r is the rolling resistance coefficient, $C_a = C_{a,0} + k \cdot \left(A_f / A_{ref} \right)$ is the

coefficient of aerodynamic force, k is a correction factor depending on specific vehicle characteristics, A_{ref} is a standard reference surface used to normalize A_f [13]-[15]. $C_x = C_{x,0} + k\left(L/H\right)$, $C_y = C_{y,0} \cdot \left(t/L\right) \cdot \sin\psi$, and $C_z = C_{z,0} + k_1 \cdot \left(A_{roof}/A_f\right) + k_2 \cdot \left(A_{spoiler}/A_f\right)$ are longitudinal, lateral and vertical force coefficients. k_1 and k_2 are correction factors for roof shape and aerodynamic devices, A_{roof} is the roof area and $A_{spoiler}$ is the spoiler area [1] [5] [14] [15]. $C_l = C_{l,0} + k_l \cdot \left(h/t\right)$, $C_m = C_{m,0} + k_m \cdot \left(d/L\right)$ and $C_n = C_{n,0} + k_n \cdot \left(L/t\right)$ are rolling, pitching and yawing moment coefficients, h is the height of the vehicle's center of gravity, d is the distance between the center of pressure and the center of gravity, k_m and k_n are the pitching and yawing moment correction factors [5] [11] [15].

2.2. Constraints Formulation

The constraints arising from the modeling of our problem concern constraints on the safety of the vehicle, driver and passengers on board, technological constraints, operational constraints, speed, roll angle, yaw angle and control position. These constraints are expressed in terms of the following boundary conditions [9]:

1) Longitudinal vehicle position is bounded by $X_0^o \le X_G^o \le X_f^o$ where X_0^o, X_f^o are longitudinal position limits. The lateral vehicle position is bounded by $Y_0^o \le Y_G^o \le Y_f^o$ where Y_0^o, Y_f^o are lateral positions limits and the vertical vehicle position is bounded by $Z_0^o \le Z_G^o \le Z_f^o$ where Z_0^o, Z_f^o are the vertical positions limits.

2) The aerodynamic velocity of the vehicle v_a must be bounded by $v_{\min} \le v_a \le v_{\max}$ where $v_{\min}$ and $v_{\max}$ are limits of the vehicle aerodynamic velocity. Vehicle acceleration γ_a is given by $a_{\min} \le \gamma_a \le a_{\max}$ where $a_{\min}$ and $a_{\max}$ are limits of the vehicle acceleration.

3) Constraints on longitudinal velocity of the vehicle $u_{\min} \le u \le u_{\max}$, lateral velocity of the vehicle $v_{\min} \le v \le v_{\max}$ and vertical velocity of the vehicle $w_{\min} \le w \le w_{\max}$.

4) Constraints on vehicle roll speed $p_0 \le p \le p_f$, vehicle pitching speed $q_0 \le q \le q_f$ and the vehicle yaw rate $r_0 \le r \le r_f$ should also be taken into account. Nautical angles also vary: roll angle $\theta \in \left[\theta_0, \theta_f\right]$, pitch angle $\phi \in \left[\phi_0, \phi_f\right]$ and yaw angle $\psi \in \left[\psi_0, \psi_f\right]$.

5) Command $\delta\left(t\right)$ of the vehicle is bounded between the limits δ_{x_0} and δ_{x_f} for thrust control, δ_{l_0} and δ_{l_f} for roll control, δ_{m_0} and δ_{m_f} for pitch control and δ_{n_0} and δ_{n_f} for yaw control.

6) The vehicle mass varies in the mobile frame: $m_f \le m \le m_0$. This constraint results in fuel consumption, the thrust of the vehicle and the addition of passengers or goods [9].

On the whole, the constraints come together in the following connection:

$$l_1\left(y,\delta\right) \le 0,\ l_2\left(y,\delta\right) \ge 0 \tag{4}$$

where $l\left(t\right): \mathbb{R}^{15} \times \mathbb{R}^4 \to \mathbb{R}^{15} \times \mathcal{U}, \left(y,\delta\right) \mapsto l\left(y,\delta\right)$

$$
\begin{aligned}
l_1(y,\delta) = \big(&m(t)-m_f, v_a(t)-v_{af}, \gamma_a(t)-\gamma_{af}, u(t)-u_f, v(t)-v_f,\\
&w(t)-w_f, p(t)-p_f, q(t)-q_f, r(t)-r_f, \theta(t)-\theta_f, \phi(t)-\phi_f,\\
&\psi(t)-\psi_f, X_G^o(t)-X_f^o, Y_G^o(t)-Y_f^o, Z_G^o(t)-Z_f^o\\
&\delta_x(t)-\delta_{xf}, \delta_l(t)-\delta_{lf}, \delta_m(t)-\delta_{mf}, \delta_n(t)-\delta_{nf}\big)\\
l_2(y,\delta) = \big(&m(t)-m_0, v_a(t)-v_{a0}, \gamma_a(t)-\gamma_{a0}, u(t)-u_0, v(t)-v_0,\\
&w(t)-w_0, p(t)-p_0, q(t)-q_0, r(t)-r_0, \theta(t)-\theta_0, \phi(t)-\phi_0,\\
&\psi(t)-\psi_0, X_G^o(t)-X_0^o, Y_G^o(t)-Y_0^o, Z_G^o(t)-Z_0^o\\
&\delta_x(t)-\delta_{x0}, \delta_l(t)-\delta_{l0}, \delta_m(t)-\delta_{m0}, \delta_n(t)-\delta_{n0}\big)
\end{aligned}
$$

2.3. Objective Function Formulation

The main goal of this work is to optimize the fluidity of road traffic. This flow traffic function is defined as the measure of a road network's ability to allow for the efficient and uninterrupted movement of vehicles. This function promotes smoother traffic flow. High fluidity implies rapid and unimpeded movement, while low fluidity indicates congestion, frequent stops, and interruptions in the flow of traffic.

To model the traffic fluidity function, we introduce $V(y,t)$ as the total circulation speed of the flow of vehicles, which takes into account the contributions of the components of the aerodynamic speed transformed by the aerodynamic angles together with the effects of rotation [16]-[18]. The traffic fluidity function is then modeled as follows:

$$J(y,\delta,t) = \frac{1}{v_{\max}^2}\left\| R(\phi,\theta,\psi)v_a + \Omega \times r_G^o \right\|^2 + g(y,\delta), \tag{5}$$

where $R(\phi,\theta,\psi)$ is the rotation matrix, $v_a = (u,v,w)^{\mathrm{T}}$ is the vehicle aerodynamic speed, $\Omega = (p,q,r)^{\mathrm{T}}$ is the vehicle rotation speed vector and $r_G^o = \left(X_G^o, Y_G^o, Z_G^o\right)^{\mathrm{T}}$ is the vehicle position in the mobile frame R_G relative to the observator frame R_O, $g(y,\delta) = \dfrac{\|\delta\|^2}{\delta_{\max}^2}$ is the control price function [17] [19], and $y = \left(m, v_a, \gamma_a, u, v, w, p, q, r, \theta, \phi, \psi, X_G^o, Y_G^o, Z_G^o\right)$ is the state vector.

The form (5) above is chosen as the most suitable in the concept of traffic optimization because it takes into account aerodynamics, which influences the dynamic performance of the vehicle in traffic; the vehicle orientation matrix, which allows for changes in direction and inclination, essential for smooth movement in varied conditions; and the costs associated with control decisions.

The conceptual definition of traffic fluidity and the mathematical form (5) allow for effective modeling of traffic dynamics while incorporating practical and theoretical considerations, making it a valuable tool for traffic optimization. To support this approach, we can refer to pioneering works that laid the foundations for traffic flow by linking speed to traffic density and mathematical models that link speed and density, reinforcing the idea that traffic flow is a function of these parameters [20] [21].

2.4. Explicit Formulation of the Road Traffic Flow Dynamics

By combining dynamic modelling (3), constraints formulation in section 1 and the objective function (5), the nonlinear mathematical traffic optimization model is given as follows:

$$\max_{(y,\delta)\in\mathbb{R}^{15}_{ad}\times\mathcal{U}_{ad}} J(y,\delta,t)=\frac{1}{v_{\max}^2}\left\|R(\phi,\theta,\psi)v_a+\Omega\times r_G^o\right\|^2+\frac{\|\delta\|^2}{\delta_{\max}^2}$$

$$s.c:\begin{cases}
\dot{m}=-\left(C_{cse}\times\tau\times\left[\dfrac{P_i\left(v_e+\alpha_1\delta_x\right)}{LHV_{fuel}\cdot\eta_m\cdot\eta_c}+\left(p_0-p_e\right)\cdot A_e\right]\right)^{\frac{1}{2}}\\
\dot{v}_a=\dfrac{1}{2m}\rho A_f C_a\left(v_a+v_{wind}\right)^2+C_r g\cos\theta\\
\dot{\gamma}_a=-\dfrac{\dot{m}}{2m^2}\rho A_f C_a\left(v_a+v_{wind}\right)^2+\dfrac{1}{m}\rho A_f C_a\dot{v}_a\left(v_a+v_{wind}\right)-C_r g\dot{\theta}\sin\theta\\
\dot{u}=\dfrac{1}{m}\left[-mg\sin\theta-\dfrac{1}{2}\rho A_f\left(u+u_w\right)^2C_x-C_r mg\cos\theta+F_x-\dot{m}u-m\left(qw-rv\right)\right]\\
\dot{v}=\dfrac{1}{m}\left[mg\cos\theta\sin\phi+\dfrac{1}{2}\rho A_f\left(v+v_w\right)^2C_y+F_y-\dot{m}v-m\left(ru-pw\right)\right]\\
\dot{w}=\dfrac{1}{m}\left[mg\cos\theta\cos\phi+\dfrac{1}{2}\rho A_f\left(w+w_w\right)^2C_z+F_z-mg\cos\theta-\dot{m}w-m\left(pv-qu\right)\right]\\
\dot{p}=\dfrac{C}{AC-D^2}\left[\dfrac{1}{2}\rho A_f t\left(u+u_w\right)^2C_l+\left(B-C\right)qr+Dpq\right]\\
\quad+\dfrac{D}{AC-D^2}\left[\dfrac{1}{2}\rho A_f L\left(w+w_w\right)^2C_n+\left(A-B\right)pq-Dqr\right]+\alpha_2\delta_l\\
\dot{q}=\dfrac{1}{B}\left[\dfrac{1}{2}\rho A_f L\left(v+v_w\right)^2C_m+\left(C-A\right)pr-D\left(p^2-r^2\right)\right]+\alpha_3\delta_m\\
\dot{r}=\dfrac{A}{AC-D^2}\left[\dfrac{1}{2}\rho A_f L\left(w+w_w\right)^2C_n+\left(A-B\right)pq-Dqr\right]\\
\quad+\dfrac{D}{AC-D^2}\left[\dfrac{1}{2}\rho A_f t\left(u+u_w\right)^2C_l+\left(B-C\right)qr+Dpq\right]+\alpha_4\delta_n\\
\dot{\phi}=p+q\tan\theta\sin\phi+r\tan\theta\cos\phi,\dot{\theta}=q\cos\phi-r\sin\phi,\\
\dot{\psi}=q\dfrac{\sin\phi}{\cos\theta}+r\dfrac{\cos\phi}{\cos\theta}\\
\dot{X}_G^o=u\cos\psi-v\sin\psi,\dot{Y}_G^o=u\cos\psi+v\sin\psi,\dot{Z}_G^o=w
\end{cases}\tag{6}$$

The simplified notation of NLP (6) above is expressed as follows:

$$\max_{(y,\delta)\in\mathbb{R}^{15}_{ad}\times\mathcal{U}_{ad}} J(y,\delta)$$

$$s.c:\begin{cases}\dot{y}=f\left(t,y,\delta\right)\\ t_0\le t\le t_f\\ t_0=0,\ y(0)=y_0,\ \delta(0)=\delta_0\\ l_1\left(y,\delta\right)\le 0,\ l_2\left(y,\delta\right)\ge 0\end{cases}\tag{7}$$

where $y:\left[t_0,t_f\right]\to\mathbb{R}^{15}$ is the state vector, and $\delta:\left[t_0,t_f\right]\to\mathcal{U}\subset\mathbb{R}^4$, $f:\left[t_0,t_f\right]\to\mathbb{R}^{15}\times\mathcal{U}$.

Although this paper discusses a model that optimizes the trajectory of a single vehicle and focuses on individual parameters, its effects are felt throughout the overall traffic system. By improving the behavior of one vehicle, we contribute not only to its own efficiency but also to the traffic flow of other vehicles, creating a more fluid and organized traffic environment. This holistic approach is essential for developing sustainable and effective urban traffic management solutions.

3. Digital Processing of the Model

The proposed model as defined in relation (7) is a controlled nonlinear problem. A fourth-order digital Runge-Kutta method is used to discretize and solve the system of nonlinear differential equations. This RK4 method is chosen because of its higher order while avoiding the disadvantages of other methods, which require evaluation of the partial derivatives of f [5].

RK4 Algorithm:

1) Let's fix the number N of iterations and the time interval $\left[t_0, t_f\right]$, and calculate the step $h = t_{n+1} - t_n = \dfrac{t_f - t_0}{N}$ for each differential equation.

2) For $0 \le n \le N$

$$\max_{(y,\delta)\in\mathbb{R}^{15}_{ad}\times\mathcal{U}_{ad}} J\left(y,\delta,t\right)$$

$$k_1 = hf\left(t_n, y_n, \delta\right)$$

$$k_2 = hf\left(t_n + \frac{h}{2}, y_n + \frac{k_1}{2}, \delta\right)$$

$$k_3 = hf\left(t_n + \frac{h}{2}, y_n + \frac{k_2}{2}, \delta\right)$$

$$k_4 = hf\left(t_n + h, y_n + k_3, \delta\right),$$

$$t_{n+1} = t_n + h$$

$$\mu_1 l_1\left(y\left(t_n\right), u\left(t_n\right), t_n\right) = 0$$

$$\mu_2 l_2\left(y\left(t_n\right), u\left(t_n\right), t_n\right) = 0,$$

$$\mu_1 \le 0,\ \mu_2 \ge 0$$

3) Updating y variables values: $y_{n+1} = y_n + \dfrac{1}{6}\left(k_1 + 2k_2 + 2k_3 + k_4\right)$

Now, the discretized NLP of (7) is expressed as follows:

$$\max_{(y,\delta)\in\mathbb{R}^{15}_{ad}\times\mathcal{U}_{ad}} \sum_{n=1}^{N} J\left(y_n, \delta_n\right)$$

$$s.c: \begin{cases} y_{n+1} = y_n + h.f\left(t_n, y_n, \delta_n\right) \\ \mu_1 l_1\left(y\left(t_n\right), u\left(t_n\right), t_n\right) = 0, \\ \mu_2 l_2\left(y\left(t_n\right), u\left(t_n\right), t_n\right) = 0 \\ \mu_1 \le 0,\ \mu_2 \ge 0 \end{cases} \tag{8}$$

Model data:

The Model parameter values and state variable limits are given in the following tables. See Table 1 and Table 2.

Table 1. Model parameter values [5] [13] [18] [22].

Denomination	Notation	Value
Fuel consumption coefficient	C_{cse}	1×10^{-4} kg.m^{-1}
Internal motor power	P_i	$\approx 2 \times 10^5$ W
Throttle ejection speed	v_e	≈ 30 m.s^{-1}
Calorific value of fuel	LHV_{fuel}	42.7×10^6 J.kg^{-1}
Motor mechanical efficiency	η_m	≈ 0.9
Fuel conversion efficiency	η_c	≈ 0.4
Environmental pressure	p_0	1.01325×10^5 Pa
Gas outlet pressure	p_e	1.0×10^5 Pa
Exhaust outlet surface	A_e	≈ 0.1 m^2
Air density	ρ	≈ 1.225 kg.m^{-3}
Vehicle frontal area	A_f	≈ 2.89 m^2
Gravity acceleration	g	≈ 9.81 m/s^2
Basic longitudinal drag coefficient	C_{x_0}	≈ 0.34
Rolling resistance coefficient	C_r	≈ 0.015
Facteur de correction	k	≈ 0.2
Correction factor for a roof form	k_1	≈ 0.05
Correction factor for aerodynamic devices	k_2	≈ 0.1
Reference surface	A_{ref}	≈ 2.6 m^2
Roof surface	A_{roof}	≈ 2 m^2
Spoiler surface	$A_{spoiler}$	≈ 0.3 m^2
Vehicle length	L	4.84 m
Vehicle width	t	1.885 m
Vehicle height	H	1.845 m
Height of vehicle of gravity center		≈ 0.5 m
Motor efficiency	η_m	≈ 0.9
Basic aerodynamic drag coefficient	C_{a_0}	≈ 0.35
Basic lateral force coefficient h	C_{y_0}	≈ 0.1
Basic vertical force coefficient	C_{z_0}	≈ -0.1
Basic roll moment coefficient	C_{l_0}	≈ 0.1
Roll moment correction factor	k_l	≈ 0.2
Basic pitch moment coefficient	C_{m_0}	≈ -0.1
Pitch moment correction factor	k_m	≈ 0.01

Continued

Basic yaw moment coefficient	C_{n_0}	≈0.02
Yaw moment correction factor	k_n	≈0.01
Pressure's center and gravity's center distance	d	≈1.2
Maximum speed allowed	$v_{\max}$	60 m.s^{-1}
3*The vehicle inertia moments	I_{xx}	1.417525 × 10^3 kgm^{-2}
	I_{yy}	5.415145 × 10^3 kgm^{-2}
	I_{zz}	5.41138 × 10^3 kgm^{-2}
Thrust control coefficient	α_1	1.5
Roll control coefficient	α_2	$1/I_{xx}$
Pitch control coefficient	α_3	$1/I_{yy}$
Yaw control coefficient	α_4	$1/I_{zz}$

Table 2. Limit values for dynamic variables [5] [13] [18] [22].

Constraint denomination	Minimum value	Maximum value
Mass of the vehicle	$m_0 \approx 3000$ kg	$m_f \approx 2500$ kg
Aerodynamic vehicle speed	$v_{a_0} = 22\ \text{m}\cdot\text{s}^{-1}$	$v_{a_f} = 55\ \text{m}\cdot\text{s}^{-1}$
Aerodynamic vehicle acceleration	$\gamma_{a_0} = -2\ \text{m}\cdot\text{s}^{-2}$	$\gamma_{a_f} = 5\ \text{m}\cdot\text{s}^{-2}$
Longitudinal vehicle speed	$u_0 = 22\ \text{m}\cdot\text{s}^{-1}$	$u_f = 50\ \text{m}\cdot\text{s}^{-1}$
Lateral vehicle speed	$v_0 = -5\ \text{m}\cdot\text{s}^{-1}$	$v_f = 5\ \text{m}\cdot\text{s}^{-1}$
Vertical vehicle speed	$w_0 = -3\ \text{m}\cdot\text{s}^{-1}$	$w_f = 3\ \text{m}\cdot\text{s}^{-1}$
Vehicle roll velocity	$p_0 = -5^\circ\cdot\text{s}^{-1}$	$p_f = 5^\circ\cdot\text{s}^{-1}$
Vehicle pitch velocity	$q_0 = -2^\circ\cdot\text{s}^{-1}$	$q_f = 2^\circ\cdot\text{s}^{-1}$
Vehicle yaw velocity	$r_0 = -2^\circ\cdot\text{s}^{-1}$	$r_f = 2^\circ\cdot\text{s}^{-1}$
Vehicle thrust control	$\delta_{x_0} = 0.1$	$\delta_{x_f} = 0.8$
Vehicle roll control	$\delta_{l_0} = -0.0275$	$\delta_{l_f} = 0.0275$
Vehicle pitch control	$\delta_{m_0} = 0$	$\delta_{m_f} = 0.095$
Vehicle yaw control	$\delta_{n_0} = -0.036$	$\delta_{n_f} = 0.35$
Roll angle	$\theta_0 = -15^\circ$	$\theta_f = 15^\circ$
Pitch angle	$\phi_0 = -30^\circ$	$\phi_f = 30^\circ$
Yaw angle	$\psi_0 = 0^\circ$	$\psi_f = 45^\circ$
Position of the vehicle's center of gravity	$X^o_{G_0} = 0$ m	$X^o_{G_f} = 10^3$ m
	$Y^o_{G_0} = -10^2$ m	$Y^o_{G_f} = 10^2$ m
	$Z^o_{G_0} = 0$ m	$Z^o_{G_f} = 10^1$ m
Limits of time	$t_0 = 0$ s	$t_f = 180$ s
Longitudinal wind speed	$u_{wind} = 4\ \text{m}\cdot\text{s}^{-1}$	
Lateral wind speed	$v_{wind} = 2.5\ \text{m}\cdot\text{s}^{-1}$	
Verticalal wind speed	$w_{wind} = 1\ \text{m}\cdot\text{s}^{-1}$	

4. Digital Results

The model is tested on the technical specifications of a Toyota Land Cruiser Lounge Pack Techno civilian vehicle, 204 ch-BVA6, 5-door/5-seater, 2.8 L D-4D Diesel and with a mass of around 3×10^3 kg. The optimality characteristics of IPOPT's output solutions are such that:

EXIT = Optimal Solution Found

Ipopt 3.8.0: Optimal Solution Found

Number of Iterations = 105

Objective function value = 2.0400987422160904e+002

Option (rel_boundtol/abs_boundtol) = 1.769176e−06/1.769172e−06

Dual infeasibility = 2.2110767346561301e−014

Constraint violation = 8.8359453712429730e−019

Complementarity = 9.0909099006618611e−010

Overall NLP error = 9.0909099006618611e−010

Number of objective function evaluations = 119

Number of objective gradient evaluations = 106

Number of equality constraint evaluations = 119

Number of inequality constraint evaluations = 119

Number of equality constraint Jacobian evaluations = 106

Number of inequality constraint Jacobian evaluations = 106

Number of Lagrangian Hessian evaluations = 105

Total CPU secs in IPOPT (w/o function evaluations) = 10.781

Total CPU secs in NLP function evaluations = 49.640

The graph in Figure 2 shows the values of the fluidity function J, mass dynamic m, aerodynamic velocity v_a and aerodynamic acceleration γ_a as a function of time, respectively. These results show that for a simulation time of 180 seconds, road traffic fluidity ranges from 0.189882 to 1.14225. This result shows average behavior and free-flowing traffic conditions where all vehicles in the traffic flow seem to follow the same speed and move at high velocities. Given this result, it can be asserted that traffic is evolving towards a fluid state. The vehicle's mass varies between 3×10^3 kg and 2.99904×10^3 kg, *i.e.* a mass loss of around 0.96 kg or 0.032% of its total mass. Now, the additional assumption of considering the mass of the moving vehicle as a variable has an important meaning when modeling road traffic dynamics.

Although the 0.032% variation in mass may seem insignificant from a numerical standpoint, its practical significance is considerable in the field of traffic flow optimization. This small variation is a critical element of the model, as it reflects complex dynamics and contributes to cumulative improvements that can have a major impact on traffic, time savings for users that translate into reduced fuel and

vehicle wear costs, and the quality of life for users. These savings can be significant when considered over an extended time scale or across a large number of vehicles. Aerodynamic speed and acceleration evolve positively from small to large values, meaning that traffic vehicles accelerate slightly for attack or climb maneuvers. These results correspond to fluid traffic situations where vehicles are moving normally.

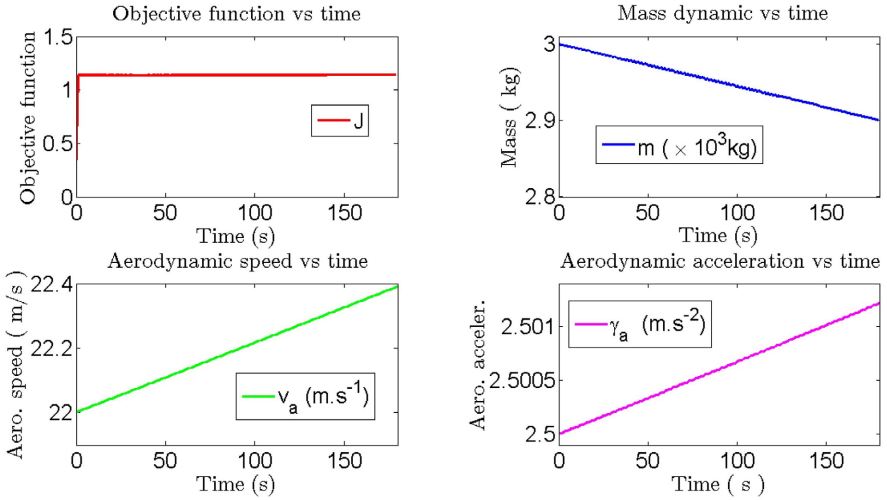

Figure 2. Objective function and vehicle mass, aerodynamic speed and acceleration.

The graphs in **Figure 3** show the optimal vehicle controls. These results show that the main thrust command δ_x varies from 0.46 to 0.1. The roll command varies between 0.0007 and 0.0017 but remains constant between 5 and 140 seconds of vehicle motion, proving vehicle stability and passenger comfort over this time interval. Pitch control decreases significantly, meaning that the nose of the vehicle lowers, causing the vehicle to descend. Yaw control increases from 0.113 to 0.16, meaning that the vehicle pivots to the right, resulting in a right turn for the time interval 0 to 177 seconds.

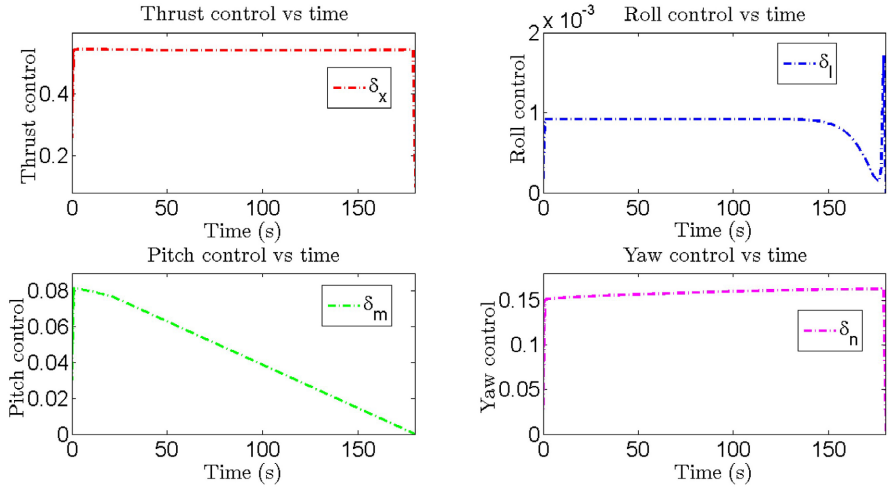

Figure 3. Vehicle dynamic controls.

Figure 4 shows an evolution of the respective longitudinal, lateral, vertical components of aerodynamic velocity and roll angle. This graph shows that the longitudinal velocity u varies from 22 m/s to 21.36 m/s, meaning that the vehicle is slowing down or braking in a straight line in the direction of its motion. The lateral velocity v evolves positively from 3 m/s to 3.72 m/s in a curved line, meaning that the vehicle is subjected to the more pronounced lateral motion on a curvilinear road. This is common on bends when the vehicle is making a sharp turn or evasive maneuver. The w vertical speed, on the other hand, varies positively from 1.5 m/s to 1.022 m/s, meaning that the vehicle is descending on a curvilinear road. Roll angle θ evolves positively from 1 to 0.86, meaning that the vehicle is returning to a stable vertical position.

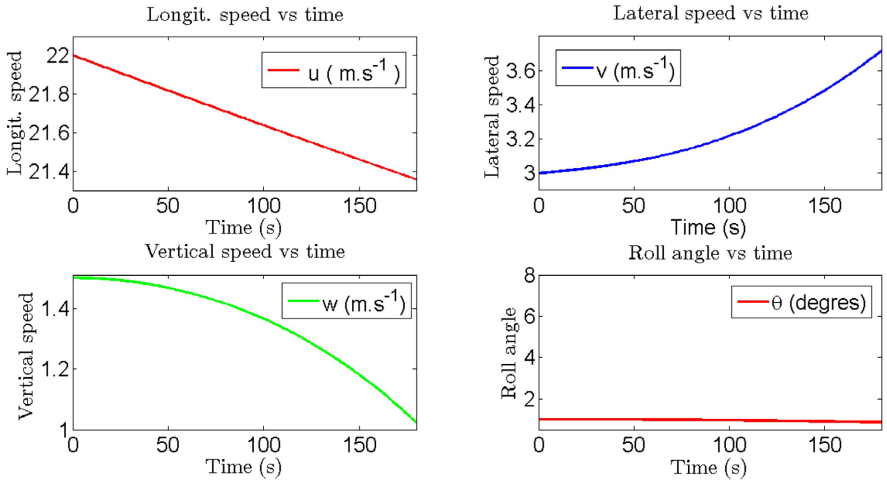

Figure 4. Vehicle speeds.

The results in Figure 5 show the evolution of the pitch and yaw angles of the vehicle's rotational movement and the evolution of p and q vehicle's rotational speed. These results show that the pitch angle ϕ evolves positively from 1 to 7.86, meaning that the vehicle is tilting upwards or maneuvering uphill. The yaw angle ψ varies positively from 1 to 1.007, implying vehicle rotation to the right. The roll speed p varies positively between 0 and 13.6/s, implying that the vehicle is rolling to the right. The pitching speed decreases from 0 to −0.3/s.

Figure 6 shows the third component r of the vehicle's rotational speed and the time evolution of the center of mass G in the R_G frame from the point of view of an observer in the R_O frame. The observation position is taken above the ground and the trajectory is as follows (50 m, 20 m, 1 m). These graphs show that the yaw rate r changes slightly from 0 to 0.04/s, implying that the vehicle rotates slightly to the right. The position X_G^o varies positively between 50 m and 71.6 m in the moving frame relative to an observer attached to the inertial frame, which indicates that the vehicle is moving forward for an observer attached to the inertial frame. The position Y_G^o evolves positively between 20 m and 23.6 m in the moving frame relative to an observer attached to the inertial frame. This indicates that

the vehicle is moving to the right relative to an observer attached to the inertial frame. The position Z_G^o varies positively between 1 m and 2.35 m in the mobile frame relative to an observer attached to the inertial frame, which means that the vehicle is climbing relative to an observer attached to the inertial frame.

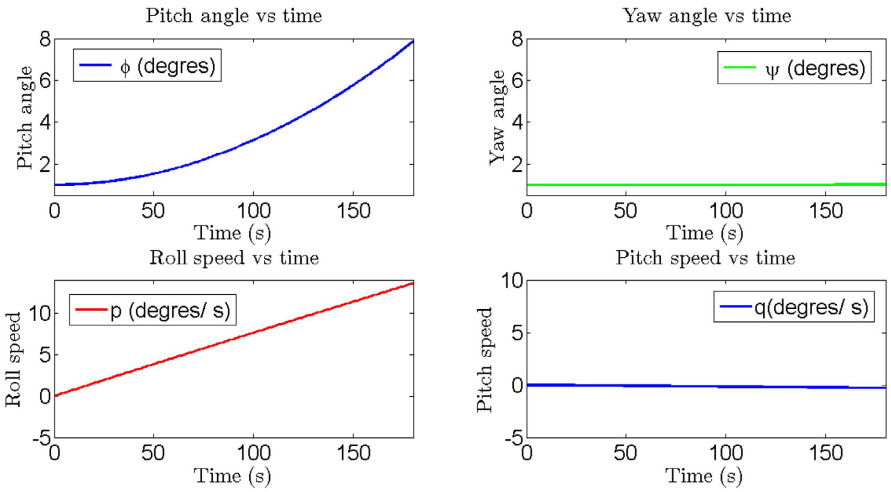

Figure 5. Vehicle nautical angles.

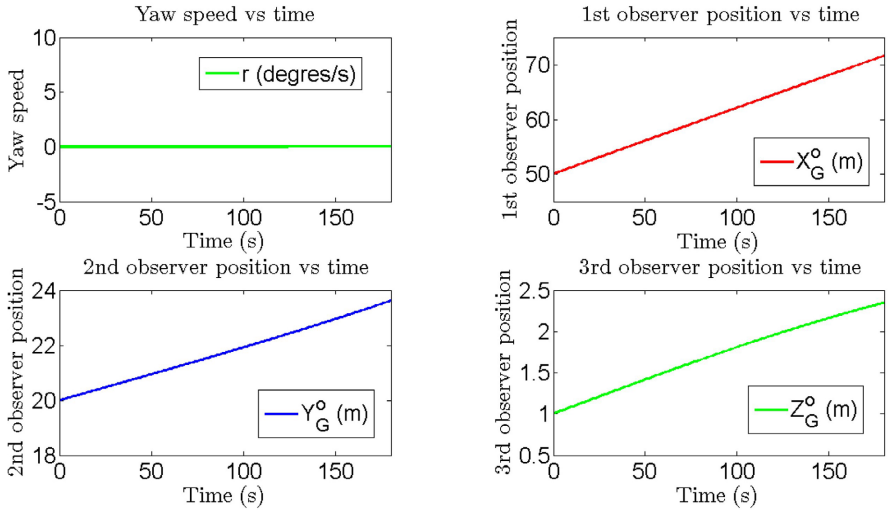

Figure 6. Observer positions.

It is important to acknowledge the limitations of our optimization model. First, the model focuses on a single vehicle and may not capture the complex, dynamic interactions that occur in a multi-vehicle environment. Additionally, the environmental conditions have been oversimplified, which may limit the model's ability to produce robust results in real-world scenarios where factors such as weather, road conditions, and traffic density influence vehicle behavior. Finally, our model relies on vehicle-specific parameters, such as those of the Toyota Land Cruiser. This may restrict generalization to other types of vehicles with different characteristics. These constraints should be considered when planning future research in this area.

5. Conclusions

In this work, a mathematical model has been developed for traffic road optimization. This model aims to maximize traffic flow under dynamic, control, operational and technical constraints. An RK4 algorithm has been developed to solve the optimization problem under inter-coupled nonlinear dynamic constraints. This method is used to discretize the problem because of its high-order efficiency in solving nonlinear differential equations. The IPOPT solver coupled with the AMPL programming language was used to extract the optimal solution from the model. The results obtained here for the traffic dynamics constraints and the objective fluidity function prove that our model can optimize traffic conditions on a road infrastructure toward totally fluid traffic.

The new hypothesis of mass variation, in particular, the decrease in the mass of a moving vehicle allows us to model scenarios in which traffic demand fluctuates. This facilitates the dynamic adjustment of resources and routes.

Optimizing traffic flow under dynamic constraints, control, and safety allows for the optimization of routes and travel times, which reduces traffic congestion. This enables traffic managers to improve the overall efficiency of the road network, ensure user safety, and better anticipate and respond to changes in traffic conditions.

This model can be used to develop control algorithms for autonomous vehicles and improve intelligent traffic management systems. It makes accurate predictions and facilitates communication between vehicles, optimizing trajectories and traffic flow. Its ability to identify congestion points reduces waiting times and prevents traffic jams. By incorporating safety features, this model enhances user safety and improves the efficiency of the road network. The application of this model can mark a step toward smarter, more sustainable transportation systems.

Future Perspectives

In this study, we considered the fluidity of a single route with a single vehicle. Our next research will extend this to the joint optimization of two vehicles' movements.

Conflicts of Interest

The authors declare no conflicts of interest regarding the publication of this paper.

References

[1] Derbel, O. (2014) Modélisation microscopique et macroscopique du trafic. Impact des véhicules automatisés sur la sécurité du conducteur. Thèse de Doctorat de l'Université de Haute-Alsace. https://tel.archives-ouvertes.fr/tel-01314140

[2] Treiber, M. and Kesting, A. (2013) Traffic Flow Dynamics: Data, Models and Simulation. Springer-Verlag, 983-1000.

[3] Treiber, M. and Kesting, A. (2012) Model-Based Traffic Flow Optimization. In: Treiber, M. and Kesting, A., Eds., *Traffic Flow Dynamics: Data, Models and Simulation*, Springer, 403-422. https://doi.org/10.1007/978-3-642-32460-4_21

[4] Li, L. (2021) Modélisation et contrôle d'un véhicule tout-terrain à deux trains directeurs. Thèse de doctorat de l'Université PSL.

[5] Duysinx, P. (2020-2021) Performance et dynamique des véhicules, LTAS-Ingénierie des Véhicules Terrestres. Université de Liège.

[6] Saafi, K. (2012) Amélioration de l'implémentation des volets dans un modèle de dynamique et contrle de vol de l'avion L1011-500. Université de Québec.

[7] Venture, G. (2003) Identification des paramètres dynamiques d'un véhicule automobile. Thèse de doctorat de l'École Centrale de Nantes et l'Université de Nantes. https://theses.hal.science/tel-00696169

[8] Duysinx, P. and Bauduin, I.S. (2021) Meca0525 Vehicle Performance and Dynamics.

[9] Nahayo, F. (2012) Modèle mathématique d'optimisation non linéaire du bruit des avions commerciaux en approche sous contrainte énergétique. Thèse de doctorat de l'Université Claude Bernard Lyon 1. https://theses.hal.science/tel-00855690v1

[10] Eraydin, E. (1994) Domaine de validité des équations de la dynamique de vol: Découplage. Thèse de l'Ecole Nationale Supérieure de l'Aéronautique et de l'Espace, ONERA-CERT.

[11] Wong, J.Y. (2022) Theory of Ground Vehicles. 5th Edition, John Wiley & Sons. https://doi.org/10.1002/9781119719984

[12] Ian Douglas, G. (2003) A New Approach to Estimate Congestion Impacts for Highway Evaluation: Effects on Fuel Consumption and Vehicle Emissions. Ph.D. Thesis, ResearchSpace@Auckland.

[13] Hucho, W.-H. (1995) Aerodynamics of Road Vehicles. *Progress in Technology*, **49**, 3-60.

[14] Boretti, A. (2019) Advances in Turbocharged Racing Engines: An SAE Technical Paper Compilation. SAE International.

[15] Gillespie, T. (2021) Fundamentals of Vehicle Dynamics. SAE international.

[16] Lieu, H. (2005) the Physics of Traffic: Empirical Freeway Pattern Features, Engineering Applications, and Theory. *Physics Today*, **58**, 54-56. https://doi.org/10.1063/1.2155762

[17] Helbing, D. (2001) Traffic and Related Self-Driven Many-Particle Systems. *Reviews of Modern Physics*, **73**, 1067-1141. https://doi.org/10.1103/revmodphys.73.1067

[18] Luu, H., Nouvelière, L. and Mammar, S. (2010) Dynamic Programming for Fuel Consumption Optimization on Light Vehicle. 6*th IFAC Symposium Advances in Automotive Control*, Munich, 12-14 July 2010, 372-377.

[19] Treiber, M. and Kesting, A. (2012) Elementary Car-Following Models. In: Treiber, M. and Kesting, A., Eds., *Traffic Flow Dynamics*: *Data*, *Models and Simulation*, Springer, 157-180. https://doi.org/10.1007/978-3-642-32460-4_10

[20] Greenshields, B.D., Bibbins, J.R., Channing, W.S. and Miller, H.H. (1935) A Study of Traffic Capacity. *Proceedings Highway Research Record*, Vol. 14, 448-477.

[21] Lighthill, M.J. and Whitham, G.B. (1955) On Kinematic Waves II. A Theory of Traffic Flow on Long Crowded Roads. *Proceedings of the Royal Society of London. Series A. Mathematical and Physical Sciences*, **229**, 317-345.

[22] Rajamani, R. (2012) Vehicle Dynamics and Control. Department of Mechanical Engineering, University of Minnesota.